Science in China Series E: Technological Sciences

A reduced-order method for estimating the stability region of power systems with saturated controls

GAN DeQiang, XIN HuanHai†, QIU JiaJu & HAN ZhenXiang

Department of Electrical Engineering, Zhejiang University, Hangzhou 310027, China

In a modern power system, there is often large difference in the decay speeds of transients. This could lead to numerical problems such as heavy simulation burden and singularity when the traditional methods are used to estimate the stability region of such a dynamic system with saturation nonlinearities. To overcome these problems, a reduced-order method, based on the singular perturbation theory, is suggested to estimate the stability region of a singular system with saturation nonlinearities. In the reduced-order method, a low-order linear dynamic system with saturation nonlinearities is constructed to estimate the stability region of the primary high-order system so that the singularity is eliminated and the estimation process is simplified. In addition, the analytical foundation of the reduction method is proven and the method is validated using a test power system with 3 buses and 5 machines.

saturation nonlinearity, power system stabilizer, linear matrix inequality, singular perturbation method, reduced-order method

1 Introduction

Saturation nonlinearities are ubiquitous since the physical actuator or sensor is subject to saturation owing to its maximum and minimum limits which are either intentionally designed or result from the limitations of equipment[1−3]. Most, if not all, power system controls are subject to saturation nonlinearities[4−6]. For example, the outputs of a PSS (power system stabilizer) and excitation control all have saturation[7−9]. As early as 1995, Mohler[10] has indicated that the performance of power system controls may not meet the expectation of control design if the controls are subjected to saturation. The assertion is not surprising, as later simulation results of ref. [8] also

Recommended by Prof. LU Qiang, member of Editorial Committee of Science in China, Series E: Technological Sciences
Received May 15, 2007; accepted June 5, 2007
doi: 10.1007/s11431-007-0073-6
†Corresponding author (email: deqiang.gan@ieee.org, eexinhh@gmail.com)
Supported by the National Natural Science Foundation of China (Grant No. 50595411) and the New Century Outstanding Investigator Program of the Ministry of Education (Grant No. NCET-04-0529)

verified it. Chinese scholars first explored the saturation control design in power systems[7,11]. In fact, any nonlinearity in a dynamic system has impact on the stability of the system[12,13]. Thus, the saturation nonlinearity in power system controls may have a nontrivial impact on power system stability. Unfortunately, this issue has long been ignored by many. Therefore, quantifying the impact of saturation nonlinearities on power system stability is a fundamental question. As such, the analytical approach from the viewpoint of the stability region is receiving more and more attention.

It is of difficulty to characterize the saturated stability region[12]. Progress, mainly based on the classical theory of Lyapunov, has been made in recent years[14,15]. In particular, the work of Hu et al.[12,16] introduced a LMI optimization to seek Lyapunov functions and the estimated stability region solution is improved. This approach was later applied to power systems[17] to evaluate the performance of a PSS. The importance of this result is that it permits a quantitative evaluation of saturated PSS performance, opening a new way to analyze the impact of control limits on power system stability.

An advantage of the above result is that it is applicable to rather general saturated linear systems. However, it could be a disadvantage. For a system with fast controls, the difference between the maximum and minimum eigenvalues can be very large[18]. Thus, the decay speeds of fast and slow manifolds are very different[19,20]. If applied to such singular systems, the above method requires a very large computational burden and it suffers some other numerical problems (such as truncation error, etc.). A power system stability model described here can exhibit the singularity[21]. This work proposes a solution to this problem.

Singular perturbation is a popular method for separating the fast and slow manifolds of dynamic systems including power systems[19,22]. To extend the results presented in refs. [12,17,23], we describe an order-reduction method for singular saturated systems. We prove that, under certain conditions, the reduced-order system produces exactly the same stability analysis result. Since the fast manifolds in a saturated system are globally stable and decay rapidly, one only needs to perform stability analysis on the reduced-order system, achieving a number of objectives, namely, elimination of the singularity and reduction of computational effort.

In this work, an order-reduction method for the singular saturated system is first introduced by taking PSS performance analysis as an example. An application of the proposed method is then described. A numerical example is presented to further illustrate the suggested result.

Nomenclature. Given any vector $\boldsymbol{x}, \boldsymbol{y} \in R^n$, $\boldsymbol{x} \leqslant (\geqslant) \boldsymbol{y}$, the elements, such as $x_i - y_i$, are (non)negative; matrix $A > 0$ ($A \geqslant 0$) means that matrix A is (semi)positive definite; symbol "$\Leftrightarrow$" means "if and only if".

2 Basic saturation model and traditional methods for its stability region estimation

2.1 Power system singular perturbation model with saturation nonlinearities

In a power system, the control system of excitation usually includes the additional signal of a PSS control system, as shown in Figure 1.

As shown in Figure 1, we consider that the excitations' and PSSs' outputs are subject to saturation nonlinearities of which the characteristics are shown in Figure 2 and described by the following saturation function in this paper.

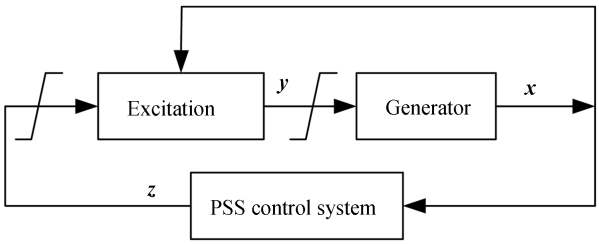

Figure 1 The control system of a generator system.

$$\mathrm{sat}_i(\eta)=\begin{cases}\eta, & |\eta|\leqslant \bar{u}_i,\\ \bar{u}_i\mathrm{sign}(\eta), & |\eta|>\bar{u}_i,\end{cases} \tag{1}$$

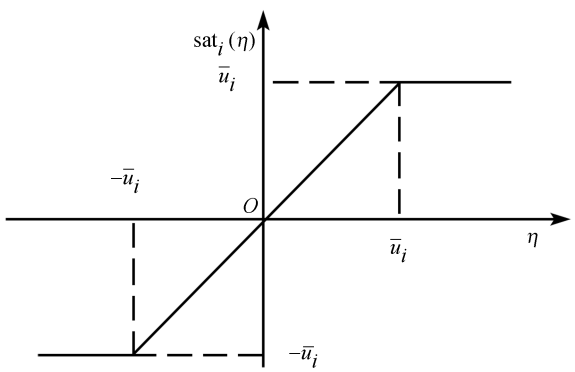

Figure 2 A saturation function.

Generally, due to the high gain and the fast transient requirement in the control systems, the decay speeds of their transients are faster than those of the generators. Thus, considering the effect of saturation nonlinearities and the large difference in the decay speeds of transients, the dynamic model for analyzing the small signal stability of a closed-loop power system can be formulated as[24]

$$\dot{\boldsymbol{x}} = A_{11}\boldsymbol{x} + A_{12}\boldsymbol{y} + A_{13}\boldsymbol{z} + B_1\mathrm{sat}(K_1\boldsymbol{y}), \tag{2}$$

$$\varepsilon\dot{\boldsymbol{y}} = A_{21}\boldsymbol{x} + A_{22}\boldsymbol{y} + A_{23}\boldsymbol{z} + B_2\mathrm{sat}(K_2\boldsymbol{z}), \tag{3}$$

$$\varepsilon\dot{\boldsymbol{z}} = A_{31}\boldsymbol{x} + A_{33}\boldsymbol{z}, \tag{4}$$

where $\boldsymbol{x}\in R^{n_1}$ denotes the state variables of generators, $\boldsymbol{y}\in R^{n_2}$ and $\boldsymbol{z}\in R^{n_3}$ are the state variables of excitation and PSS, respectively; $\varepsilon\in R^+$ is a small parameter, which denotes the large difference of decay speeds of the state variables between the control systems and the generators; $\mathrm{sat}(\cdot)$ is a saturation vector function whose expression is $\mathrm{sat}(\eta)=[\mathrm{sat}_1(\eta_1), \mathrm{sat}_2(\eta_2), \cdots\mathrm{sat}_s(\eta_s)]^{\mathrm{T}}$.

Let

$$\boldsymbol{\xi}=\begin{bmatrix}\boldsymbol{x}\\ \boldsymbol{y}\\ \boldsymbol{z}\end{bmatrix},\quad A=\frac{1}{\varepsilon}\begin{bmatrix}\varepsilon A_{11} & \varepsilon A_{12} & \varepsilon A_{13}\\ A_{21} & A_{22} & A_{23}\\ A_{31} & 0 & A_{33}\end{bmatrix}; \tag{5}$$

$$B=\begin{bmatrix}B_1 & 0\\ 0 & \varepsilon^{-1}B_2\\ 0 & 0\end{bmatrix},\quad K=\left[\begin{array}{c:c:c}0 & K_1 & 0\\ \hdashline 0 & 0 & K_2\end{array}\right]. \tag{6}$$

Thus, systems (2)—(4) can be rewritten as the following compact expression:

$$\dot{\boldsymbol{\xi}}=A\boldsymbol{\xi}+B\mathrm{sat}(K\boldsymbol{\xi}). \tag{7}$$

Define a linear set F and the stability region Ω as follows:

$$F=\{\boldsymbol{\xi}\mid -\overline{\boldsymbol{u}}\leqslant K\boldsymbol{\xi}\leqslant\overline{\boldsymbol{u}}\}, \tag{8}$$

$$\Omega=\{\boldsymbol{\xi}\mid\varphi_t(\boldsymbol{\xi})\to 0\}, \tag{9}$$

where $\overline{\boldsymbol{u}}\in R^m$ is composed of the upper-bound of the saturation function $\mathrm{sat}_i(\cdot)$, such as $\overline{u}_i$ ($i=1,2,\cdots m$), and the inequalities in eq. (8) are on the basis of element by element; $\varphi_t(\boldsymbol{\xi})$ denotes the trajectory of system (7) starting from $\boldsymbol{\xi}$. The term $\varphi_t(\boldsymbol{\xi})$ is a continuous function due to the continuity of $\mathrm{sat}(\cdot)$ [25].

In the subsequent analysis, we need two assumptions:

Assumption 1. For system (7), the origin is a hyperbolic stable equilibrium point when saturation nonlinearities are ignored and set F is not empty, i.e. $A+BK$ is a stable (Hurtiwz) matrix and $\overline{u}_i>0$ hold for all i, $i=1,2,\cdots m$.

Assumption 2. Matrices A_{22} and A_{33} are stable (Hurtiwz) matrices.

From Assumption 1, it can be concluded that the stability region Ω is not empty, but may only be a neighborhood of the origin due to the effect of saturation nonlinearities[12,25]. In addition, system (7) behaves as an asymptotically linear system only when the state variables are within set F. Outside F, the dynamic behaviors are difficult to catch directly. In fact, when designing a control system in power systems, the saturation effects are usually ignored. This leads to reduce the expected performance of a control system. Thus, it is important to analyze the stability region of a closed-loop system with saturation nonlinearities.

2.2 Traditional methods for the stability region estimation

Suppose that there exists a high-dimension ellipsoid, say Ω_0', such that Ω_0' is an invariant set of system (7) and is a subset of F. Since system (7) behaves as the corresponding linear system in set F, the trajectories starting from Ω_0' converge to the origin when Assumption 1 holds[25]. In other words, Ω_0' is a subset of the stability region of system (7). Therefore, an invariant set of system (7) in set F can be taken as the estimated stability region. This is the basic idea of the work reported in refs. [12,16].

Suppose further that the expected initial states after a transient disturbance in a power system can be contained by an ellipse as follows:

$$X_0=\{\boldsymbol{\xi}\mid\boldsymbol{\xi}^{\mathrm{T}}P_0'\boldsymbol{\xi}\leqslant\beta^2\}, \tag{10}$$

where P_0' is a (semi)positive definite symmetric matrix; $\beta>0$ is a variable.

Remark 1. For the small-signal model of a power system, though the possible initial states cannot be obtained exactly after a transient disturbance, the shape of the set (the expected set of initial states) made up of the initial states can be roughly decided. Since X_0 is an ellipse with fixed shape and variable size, we can choose an appropriate X_0 to contain the expected set of initial states. Hence, it is reasonable to assume that X_0 contains the expected set of initial states.

Clearly, the larger X_0 which can be contained by the estimated stability region is, the more initial states the estimated stability region can contain. Thus, the more powerful the saturated control system is. On the other hand, the smaller the X_0 which can be contained by the estimated stability region is, the fewer disturbances the control system can stabilize and thus the more conservative the results are. Hence, to evaluate the control system objectively, one needs to reduce the conservation in the estimation process. In short, the estimated stability region must contain the largest possible X_0, i.e. to get the largest β. In refs. [12,17], this procedure is done via an optimization which is formulated as:

$$\beta^* = \max_{P>0} \beta, \tag{11}$$

s.t. (*a*) $X_0 \subset \Omega_0' = \{\xi \mid \xi^{\mathrm{T}} P \xi < c\}$,

(b) $\Omega_0' \subset F$,

(c) $A^{\mathrm{T}} P + PA < 0$,

where constraint (a) means that the estimated Ω_0' contains set X_0 of expected initial states; constraints (b) and (c) mean that Ω_0' is in F and is an invariant set of system (7), respectively.

Using the Schur complements of matrices, the above optimization problem can be transformed into a simple LMI (Linear Matrix Equalities) optimization problem which can be solved easily[12,17]. Hence, an optimal set of problem (11), say $\Omega_0' = \{\xi \mid \xi^{\mathrm{T}} P \xi \leqslant c\}$, can contain the largest X_0 with a fixed shape and it is also the optimal stability region estimation.

3 Theories for reducing the order of the singular saturated system

In a power system, due to the existence of small parameter ε, there could be a large difference in the decay speeds of transients. System matrix A has two groups of eigenvalues with a large difference in numerical values so system (7) could be fundamentally singular. If the traditional methods in refs. [12,17] are directly used to deal with model (11), extra computational effort is required and conservative results can be expected. In this section, we will use the singular perturbation theory to reduce the order of optimization model (11) to overcome the singularity

3.1 Integral manifold theories for singular saturated systems

Suppose that matrixes $L_y(\varepsilon)$ and $L_z(\varepsilon)$ satisfy

$$\begin{cases} \Gamma_1 = A_{21} + A_{22} L_y + (A_{23} + B_2 K_2) L_z - \varepsilon L_y A_x = 0, \\ \Gamma_2 = A_{31} + A_{33} L_z - \varepsilon L_z A_x = 0, \end{cases} \tag{12}$$

where $A_x = A_{11} + A_{12} L_y + A_{13} L_z + B_1 K_1 L_y$.

Clearly Γ_1 and Γ_2 are smooth functions with respect to matrix variables L_y and L_z.

Since the matrix $\left.\dfrac{\partial(\Gamma_1,\Gamma_2)}{\partial(L_y,L_z)}\right|_{\varepsilon=0}=\left[\begin{array}{c|c} A_{22} & A_{23}+B_2K_2 \\ \hline 0 & A_{33} \end{array}\right]^{\mathrm{T}}$ is not singular by Assumption 2, it can be concluded from the implicit function theorem that[25]: there exists $\varepsilon^*>0$ such that for every $\varepsilon\in[0,\varepsilon^*]$, matrices $L_y(\varepsilon)$ and $L_z(\varepsilon)$ satisfying expression (12) exist uniquely; $L_y(\varepsilon)$ and $L_z(\varepsilon)$ are smooth functions with respect to ε. Hence, let us do the following coordinate transformation:

$$\begin{bmatrix}\boldsymbol{x}\\ \boldsymbol{y}_1\\ \boldsymbol{z}_1\end{bmatrix}=\begin{bmatrix} I & 0 & 0\\ -L_y(\varepsilon) & I & 0\\ -L_z(\varepsilon) & 0 & I\end{bmatrix}\begin{bmatrix}\boldsymbol{x}\\ \boldsymbol{y}\\ \boldsymbol{z}\end{bmatrix}. \tag{13}$$

Since $L_y(\varepsilon)$ and $L_z(\varepsilon)$ satisfy eq. (12) in the new coordinates, systems (2)—(4) is changed to

$$\dot{\boldsymbol{x}}=\left(A_{11}+A_{12}L_y+A_{13}L_z+B_1K_1L_y\right)\boldsymbol{x}+A_{12}\boldsymbol{y}_1+A_{13}\boldsymbol{z}_1+B_1q_2(\boldsymbol{x},\boldsymbol{y}_1), \tag{14}$$

$$\varepsilon\dot{\boldsymbol{y}}_1=A_{22}\boldsymbol{y}_1+A_{23}\boldsymbol{z}_1+B_2q_1(\boldsymbol{x},\boldsymbol{z}_1)-\varepsilon L_yB_1q_2(\boldsymbol{x},\boldsymbol{y}_1), \tag{15}$$

$$\varepsilon\dot{\boldsymbol{z}}_1=A_{33}\boldsymbol{z}_1-\varepsilon L_zB_1q_2\left(\boldsymbol{x},\boldsymbol{y}_1\right), \tag{16}$$

where $q_1(\boldsymbol{x},\boldsymbol{z}_1)=\mathrm{sat}\left(K_2\boldsymbol{z}_1+K_2L_z\boldsymbol{x}\right)-K_2L_z\boldsymbol{x}$, $q_2(\boldsymbol{x},\boldsymbol{y}_1)=\mathrm{sat}\left(K_1\boldsymbol{y}_1+K_1L_y\boldsymbol{x}\right)-K_1L_y\boldsymbol{x}$.

Let $\boldsymbol{x}(t)$ denote coordinates $\boldsymbol{x}$ of the trajectories of systems (14)—(16). In fact, $\boldsymbol{x}(t)$ is also dependent on parameter ε. For the simplicity of the symbols, we omit ε when no misunderstanding exists and this abbreviation is applied later as well.

In the terminology of singular perturbation theory, systems (15)—(16) is termed as the system of boundary layer[25]. The terms $\boldsymbol{y}=L_y\boldsymbol{x}$ ($\boldsymbol{y}_1=0$) and $\boldsymbol{z}=L_z\boldsymbol{x}$ ($\boldsymbol{z}_1=0$) are the integral manifolds. It can be determined that the time scale of $\boldsymbol{x}$ is t and the time scale of $\boldsymbol{y}_1,\boldsymbol{z}_1$ is $\tau=t/\varepsilon$ so when ε is small, there is large difference between the decay speeds of $\boldsymbol{y}_1,\boldsymbol{z}_1$ and $\boldsymbol{x}$. For this reason, $\boldsymbol{y}$ and $\boldsymbol{z}$ are termed as the fast variables and $\boldsymbol{x}$ is termed as the slow variable.

Define further a set F_2 as follows:

$$F_2=\left\{\boldsymbol{x}\,\middle|\,-\overline{\boldsymbol{u}}\leqslant\begin{bmatrix}K_1L_y(\varepsilon)\\ K_2L_z(\varepsilon)\end{bmatrix}\boldsymbol{x}\leqslant\overline{\boldsymbol{u}}\right\}. \tag{17}$$

Due to the special characteristics of the saturation function, we can have the following conclusions about the integral manifolds of systems (2)—(4).

Lemma 1. Suppose that the following conditions are satisfied:

(1) Assumption 1 and Assumption 2 hold;

(2) $\varepsilon>0$ is sufficiently small and $\boldsymbol{x}(t)\in F_2$ is always satisfied for $\forall t\geqslant 0$.

Then systems (15)—(16) is globally exponentially stable and its time-scale is $\tau=t/\varepsilon$. Namely, the trajectories of systems (15)—(16) satisfy

$$\left\|\boldsymbol{y}_1(t)\right\|\leqslant le^{-\gamma_1\tau},\ \left\|\boldsymbol{z}_1(t)\right\|\leqslant le^{-\gamma_1\tau}\ \text{ for }\ \forall\boldsymbol{y}_1^0\ \text{ and }\ \forall\boldsymbol{z}_1^0, \tag{18}$$

where $l > 0$ and $\gamma_1 > 0$ are constants independent of ε.

Proof. Readers can refer to ref. [26] for details.

Remark 2. As shown later, if initial state $\boldsymbol{x}(0)$ satisfies some conditions then it can be guaranteed that the second condition of this lemma holds.

Lemma 1 shows that when Assumption 1 and Assumption 2 hold and parameter ε is small enough, the integral manifolds of systems (2)—(4) are uniquely existent in set F_2. Moreover, the fast variables $\boldsymbol{y}, \boldsymbol{z}$ converge to the corresponding integral manifolds exponentially and the time-scale of the convergence is $\tau = t/\varepsilon$.

3.2 Fundamental theories for stability region estimation

Construct a low-order system as follows:

$$\dot{\boldsymbol{x}} = A_x(\varepsilon)\boldsymbol{x}, \tag{19}$$

where $A_x = A_{11} + A_{12}L_y + A_{13}L_z + B_1K_1L_y$.

The following lemma shows that A_x is a stable matrix when parameter ε is small enough.

Lemma 2. If Assumption 1 and Assumption 2 hold, then there exists $\varepsilon^* > 0$ such that A_x is a stable matrix for every $\varepsilon \in [0, \varepsilon^*]$.

Proof. Readers can refer to ref. [26] for details.

Let $\boldsymbol{x}_l(t)$ denote coordinates $\boldsymbol{x}$ of the trajectories of system (19). Thus, we can obtain the relationship between $\boldsymbol{x}(t)$ and $\boldsymbol{x}_l(t)$ based on Lemma 1 and Lemma 2.

Theorem 1. Suppose that the following conditions are satisfied:

(1) Assumption 1 and Assumption 2 hold;

(2) The initial states of system (19) and the initial states of eqs. (14)—(16) satisfy $\boldsymbol{x}(0) = \boldsymbol{x}_l(0)$;

(3) $\varepsilon > 0$ is sufficiently small and $\boldsymbol{x}(t) \in F_2$ is always satisfied for $\forall t \geqslant 0$.

Then the relationship between $\boldsymbol{x}(t)$ and $\boldsymbol{x}_l(t)$ is

$$\boldsymbol{x}(t) = \boldsymbol{x}_l(t) + O(\varepsilon), \quad \forall t \geqslant 0, \tag{20}$$

and $\boldsymbol{x}(t) \to \boldsymbol{x}_l(t)$ as $t \to \infty$;

In particular, if the third condition is changed to $\varepsilon > 0$ is sufficiently small and there exists $t' > 0$ such that $\boldsymbol{x}(t) \in F_2$ is always satisfied for $\forall t \in [0, t']$, then

$$\boldsymbol{x}(t) = \boldsymbol{x}_l(t) + O(\varepsilon), \quad \forall t \in [0, t']. \tag{21}$$

Proof. Readers can refer to ref. [26] for details.

To transform the condition $\boldsymbol{x}(t) \in F_2$ to the conditions that $\boldsymbol{x}_l(t)$, the trajectories of system (19) satisfies, we further define the following set which is a subset of F_2:

$$F_3(\varepsilon) = \left\{ \boldsymbol{x} \,\middle|\, -\sigma\overline{\boldsymbol{u}} \leqslant \begin{bmatrix} K_1L_y(\varepsilon) \\ K_2L_z(\varepsilon) \end{bmatrix} \boldsymbol{x} \leqslant \sigma\overline{\boldsymbol{u}} \right\}, \tag{22}$$

where σ is a parameter and it satisfies $0 < \sigma < 1$. For example, we can choose $\sigma = 0.95$.

When ε is sufficiently small and if $\boldsymbol{x}_l(t)$ resides in set F_3, then $\boldsymbol{x}(t)$ also resides in set F_2

due to the small error between the $\boldsymbol{x}_l(t)$ and $\boldsymbol{x}(t)$ by Theorem 1. For this reason, we can obtain the following conclusions about the stability region of systems (14)—(16).

Lemma 3. Suppose that the following conditions are satisfied:

(1) Assumption 1 and Assumption 2 hold;

(2) The initial states of system (19) and those of eqs. (14)—(16) satisfy $\boldsymbol{x}(0) = \boldsymbol{x}_l(0)$;

(3) $\varepsilon > 0$ is sufficiently small and $\boldsymbol{x}_l(t) \in F_3$ is always satisfied for $\forall t \geqslant 0$.

Then $\boldsymbol{x}(t) \in F_2$ is satisfied for $\forall t \geqslant 0$.

Proof. We use a contradiction argument. Suppose that there exists an $\varepsilon \in [0, \varepsilon^*]$ such that $\boldsymbol{x}_l(t) \in F_3$ holds for $\forall t \geqslant 0$ and $\boldsymbol{x}(t) \in F_2$ is not always satisfied. The term $\varepsilon^* > 0$ is a sufficiently small constant to be evaluated later.

Thus, since $\boldsymbol{x}(0) \in F_2$ and $\boldsymbol{x}(t)$ is continuous with respect to *t*, there exists $t' > 0$ such that $\boldsymbol{x}(t')$ crosses the boundary of set F_2, say ∂F_2, from the definition of F_2, i.e. $\boldsymbol{x}(t') \in \partial F_2$ and $\boldsymbol{x}(t) \in F_2$ when $t \leqslant t'$. Thus from Theorem 3, there exists $a_0 > 0$, independent of ε, such that

$$\| \boldsymbol{x}(t') - \boldsymbol{x}_l(t') \| \leqslant a_0 \varepsilon. \tag{23}$$

On the other side, $\boldsymbol{x}(t') \in \partial F_2$ implies that there exist some subscripts, say i, such that $|(K_1 L_y(\varepsilon)\boldsymbol{x}(t'))_i| = \bar{u}_i$ or $|(K_1 L_z(\varepsilon)\boldsymbol{x}(t'))_i| = \bar{u}_i$ hold from the definition of set F_2 where symbol $(\cdot)_i$ means the *i*-th element of a vector.

However, $\boldsymbol{x}_l(t') \in F_3$ implies that both $|(K_1 L_y(\varepsilon)\boldsymbol{x}(t'))_i| \leqslant \sigma \bar{u}_i$ and $|(K_1 L_z(\varepsilon)\boldsymbol{x}(t'))_i| \leqslant \sigma \bar{u}_i$ are satisfied. Therefore when $|(K_1 L_y(\varepsilon)\boldsymbol{x}(t'))_i| = \bar{u}_i$ holds,

$$\begin{aligned} &\| (K_1 L_y(\varepsilon))_i \| \cdot \| \boldsymbol{x}(t') - \boldsymbol{x}_l(t') \| \geqslant |(K_1 L_y(\varepsilon)\boldsymbol{x}(t'))_i - (K_1 L_y(\varepsilon)\boldsymbol{x}_l(t'))_i| \\ &\geqslant |(K_1 L_y(\varepsilon)\boldsymbol{x}(t'))_i| - |(K_1 L_y(\varepsilon)\boldsymbol{x}_l(t'))_i| \geqslant (1-\sigma)\bar{u}_i. \end{aligned} \tag{24}$$

Since $L_y(\varepsilon)$ is continuous with respect to ε, there exists a constant $b_0 > 0$ independent of ε such that $\| (K_1 L_y(\varepsilon))_i \| \leqslant b_0$ is satisfied for $\forall \varepsilon \in [0, \varepsilon']$ where $\varepsilon' > 0$ is a sufficiently small constant. Hence, from expression (34), we get

$$\| \boldsymbol{x}(t') - \boldsymbol{x}_l(t') \| \geqslant b_0^{-1}(1-\sigma)\bar{u}_i. \tag{25}$$

Similarly, we also can get $\| \boldsymbol{x}(t') - \boldsymbol{x}_l(t') \| \geqslant b_0^{-1}(1-\sigma)\bar{u}_i$ if $|(K_1 L_z(\varepsilon)\boldsymbol{x}(t'))_i| = \bar{u}_i$ is satisfied.

Hence, if ε^* satisfies $0 < \varepsilon^* \leqslant \min\{a_0^{-1} b_0^{-1}(1-\sigma)\bar{u}_i, \varepsilon'\}$, then the conclusion of (23) is contradictory to that of (25). Therefore, when ε is a sufficiently small constant ($\varepsilon \in [0, \varepsilon^*]$), $\boldsymbol{x}(t) \in F_2$ is also satisfied for $\forall t \geqslant 0$.

From this lemma, we know that when ε is small enough and if it can be guaranteed that the trajectories of system (19) do not escape from set F_3, and then the condition that Theorem 1 and Lemma 1 need can be satisfied, i.e. $\boldsymbol{x}(t) \in F_2$ holds for $\forall t \geqslant 0$. When ε is small enough, Lemma 2 guarantees that for system (19) there exists an invariant set, say Ω_0, in set F_3, i.e. $\boldsymbol{x}_l(t) \in F_3$ holds for $\forall t \geqslant 0$ if $\boldsymbol{x}_l(0) \in \Omega_0$. Hence, the condition that $\boldsymbol{x}(t) \in F_2$ holds for

$\forall t \geqslant 0$ does indeed hold. Based on this condition, we can obtain the following conclusions about the stability region of systems (14)—(16).

Theorem 2. Suppose that the following conditions are satisfied:

(1) Assumption 1 and Assumption 2 hold;

(2) Parameter σ satisfies $0 < \sigma < 1$;

(3) Set Ω_0 is an invariant set of system (19) and a subset of F_3.

Then there exists $\varepsilon^* > 0$ such that for every $\varepsilon \in [0, \varepsilon^*]$, $\bar{\Omega} = \Omega_0 \times \Omega_{yz}$ is a subset of the stability region of systems (14)—(16). Here, Ω_{yz} is a large enough bounded set of $n_2 + n_3$ dimension.

Proof. For system (19), since Ω_0 is an invariant set in F_3 and when ε is small enough, matrix A_x is stable from Lemma 2. Thus, Ω_0 is a subset of the stability region of system (19)[12,17], i.e. for $\forall \boldsymbol{x}^0 \in \Omega_0$, $\boldsymbol{x}_l(t) \in \Omega_0$ and $\boldsymbol{x}_l(t) \to 0$ as $t \to \infty$. Moreover, when ε is small enough, $\boldsymbol{x}(t) \in F_2$ holds for $\forall t \geqslant 0$ from Lemma 3. For an initial state $\boldsymbol{x}(0) = \boldsymbol{x}^0 \in \Omega_0$, we get that $\boldsymbol{x}(t) \to \boldsymbol{x}_l(t)$ as $t \to \infty$ from Theorem 1. Hence, we get $\boldsymbol{x}(t) \to 0$ as $t \to \infty$ for every $\boldsymbol{x}(0) = \boldsymbol{x}^0 \in \Omega_0$ when ε is small enough.

Since set Ω_0 is an invariant set of system (19), $\boldsymbol{x}(t) \in F_2$ is satisfied for $\forall \boldsymbol{x}^0 = \boldsymbol{x}_l(0) \in \Omega_0$ from Lemma 3 when ε is small enough. Thus, we get $(\boldsymbol{y}_1(t), \boldsymbol{z}_1(t)) \to (0,0)$ as $t \to \infty$ for $\forall (\boldsymbol{y}_1^0, \boldsymbol{z}_1^0) \in \Omega_{yz}$ from Theorem 1 when ε is small enough.

Summarizing the previous analysis, when ε is small enough, for $\forall (\boldsymbol{x}^0, \boldsymbol{y}_1^0, \boldsymbol{z}_1^0) \in \Omega_0 \times \Omega_{yz}$, the trajectories $[\boldsymbol{x}(t), \boldsymbol{y}_1(t), \boldsymbol{z}_1(t)]$ of high dimension systems (14)—(16) will converge to the origin. In other words, there exists $\varepsilon^* > 0$ such that for every $\varepsilon \in [0, \varepsilon^*]$, $\bar{\Omega} = \Omega_0 \times \Omega_{yz}$ is a subset of the stability region of systems (14)—(16).

From this theorem, when ε is small, if $\Omega_0 \subset F_3$ is an invariant set of system (19), then $\bar{\Omega} = \Omega_0 \times \Omega_{yz}$ is a subset of the stability region of systems (14)—(16). Therefore, the stability region estimation of (14)—(16) can be changed to finding an invariant set Ω_0 in F_3 based on the constructed system (19). Since Assumption 1 holds from Lemma 2, the changed problem is just what refs. [12] and [17] study, i.e. to find an invariant using the LMI optimization method.

3.3 Theories for reducing the order of the set of initial states

Consider expression (10) again, i.e. the expected initial states of system (2)—(4) reside in the following $n_1 + n_2 + n_3$ dimension ellipse:

$$X_0 = \{\boldsymbol{\xi} \in R^{n_1+n_2+n_3} \mid \boldsymbol{\xi}^{\mathrm{T}} P_0' \boldsymbol{\xi} \leqslant \beta^2\}. \tag{26}$$

Perform the following transformation:

$$\boldsymbol{\xi}_1 = \boldsymbol{x}, \quad \boldsymbol{\xi}_2 = [\boldsymbol{y}_1^{\mathrm{T}}, \boldsymbol{z}_1^{\mathrm{T}}]^{\mathrm{T}}, \quad L_{yz} = [L_y^{\mathrm{T}}, L_z^{\mathrm{T}}]^{\mathrm{T}}. \tag{27}$$

From eqs. (10), (13) and (27), X_0 under the new coordinates, $(\boldsymbol{\xi}_1, \boldsymbol{\xi}_2)$ can be expressed as

$$X_0 = \left\{ \xi' \middle| \xi'^{\mathrm{T}} P_0 \xi' \leqslant \beta^2 \right\} = \left\{ \begin{bmatrix} \xi_1 \\ \xi_2 \end{bmatrix} \in R^{n_1+(n_2+n_3)} \middle| \begin{bmatrix} \xi_1 \\ \xi_2 \end{bmatrix}^{\mathrm{T}} \begin{bmatrix} P_{11}^0 & P_{12}^0 \\ P_{21}^0 & P_{22}^0 \end{bmatrix} \begin{bmatrix} \xi_1 \\ \xi_2 \end{bmatrix} \leqslant \beta^2 \right\}, \tag{28}$$

where $\xi' = \begin{bmatrix} \xi_1 \\ \xi_2 \end{bmatrix}$, $P_0 = \begin{bmatrix} P_{11}^0 & P_{12}^0 \\ P_{21}^0 & P_{22}^0 \end{bmatrix}$, $P_0' = \begin{bmatrix} P_{11}'^0 & P_{12}'^0 \\ P_{21}'^0 & P_{22}'^0 \end{bmatrix}$, $P_{11}^0 = P_{11}'^0 + 2P_{12}'^0 L_{yz} + L_{yz}^{\mathrm{T}} P_{22}'^0 L_{yz}$,

$P_{12}^0 = (P_{21}^0)^{\mathrm{T}} = P_{12}'^0 + L_{yz}^{\mathrm{T}} P_{22}'^0$, $P_{22}^0 = P_{22}'^0$.

From the conclusion in the above sub-section, we know that the estimation process of the stability region of systems (14)—(16) can be changed to finding an invariant set in F_3 based on system (19). For this reason, similar to the methods in refs. [12,17], an optimization model for estimating the stability region of system (19) with the least degree of conservatism can be formulated as

$$\beta^* = \max_{\boldsymbol{P}_x > 0} \beta. \tag{29}$$

s.t. (a) $X_0 \subset \Omega_0 \times \Omega_{yz} = \{\boldsymbol{x} \mid \boldsymbol{x}^{\mathrm{T}} P_x \boldsymbol{x} \leqslant c\} \times \Omega_{yz}$,

(b) $\Omega_0 \subset F_3$,

(c) $A_x^{\mathrm{T}} P_x + P_x A_x < 0$,

where $\Omega_{\mathbf{yz}} \in R^{n_2+n_3}$ is an arbitrary bounded set; constraint (a) means that the X_0 is in the estimated stability region; constraints (b) and (c) mean that for system (19), Ω_0 is an invariant in F_3.

In problem (29), constraint (a) corresponds to the inequalities of the high dimension, so we further introduce the following lemma to simplify it.

Lemma 4. Suppose $E(P,\rho) = \left\{ \begin{bmatrix} \xi_1 \\ \xi_2 \end{bmatrix} \middle| \begin{bmatrix} \xi_1 \\ \xi_2 \end{bmatrix}^{\mathrm{T}} \begin{bmatrix} P_{11} & P_{12} \\ P_{12}^{\mathrm{T}} & P_{22} \end{bmatrix} \begin{bmatrix} \xi_1 \\ \xi_2 \end{bmatrix} \leqslant \rho \right\}$ is a high-dimension ellipse whose projections on coordinate ξ_1 is denoted by $E_{\xi_1}(P,\rho)$. Then the following conclusions are satisfied:

(1) $E_{\xi_1}(P,\rho)$ is still an ellipse whose analytical expression is $E_{\xi_1} = \{\xi_1 \mid \xi_1^{\mathrm{T}} (P_{11} - P_{12}^{\mathrm{T}} P_{22}^{-1} P_{12}) \xi_1 \leqslant \rho\}$;

(2) $E(P,\rho) \subset E(P_1,\rho_1) \times \Omega_{\xi_2}$ if and only if $E_{\xi_1}(P,\rho) \subset E(P_1,\rho_1)$ and ξ_2 is bounded where the dimension of $E(P_1,\rho_1)$ is the same as that of ξ_1 and Ω_{ξ_2} is a large enough and bounded set.

Proof. We omit this process. Readers can refer to ref. [26].

From Lemma 3, the constraint (a) in optimization problem (29) can be changed to

$$X_0 \subset \Omega_0 \times \Omega_{yz} \Leftrightarrow E(P_1^0, \beta) \subset \Omega_0 \Leftrightarrow \beta^{-2} P_1^0 - c^{-1} P_x > 0, \tag{30}$$

where $P_1^0 = P_{11}^0 - P_{12}^0 (P_{22}^0)^{-1} P_{21}^0$, $P_{11}^0 \in R^{n_1 \times n_1}$, $P_{12}^0 \in R^{n_1 \times n_2}$, $P_{21}^0 \in R^{n_2 \times n_1}$ and $P_{22}^0 \in R^{n_2 \times n_2}$ are

the partial matrices of P_0 in expression (28), i.e. $P^0 = \left[\begin{array}{c:c} P_{11}^0 & P_{12}^0 \\ \hdashline P_{21}^0 & P_{22}^0 \end{array}\right]$.

It is worth noting that if set X_0 containing the expected initial states is not an ellipse but a polytype, we can also obtain a similar conclusion as that of Lemma 3. For this case, we do not discuss it further in this paper.

4 Reduced-order method for estimating the stability region

4.1 Reduced-order optimization model for stability region estimation

Summarizing the analysis in section 3, when ε is small enough, the traditional method for estimating the stability region can be changed to a reduced-order optimization model as follow:

$$\beta_x^* = \max_{\boldsymbol{P}_x>0} \beta_x \tag{31}$$

s.t. (a) $\beta_x^{-2} P_1^0 - c^{-1} P_x > 0$,

(b) $\Omega_0 \subset F_3$,

(c) $A_x^{\mathrm{T}} P_x + P_x A_x < 0$.

Perform a change of variables as follow:

$$\gamma_x = \beta_x^{-2}, \quad R_x = c^{-1} P_x . \tag{32}$$

By the Schur complements of matrices and eq. (32), optimization problem (31) can be transformed to the following LMI convex optimization[12,17]:

$$\gamma_x^* = \min_{\boldsymbol{R}_x>0} \gamma_x . \tag{33}$$

s.t. (a) $\gamma_x P_1^0 - R_x > 0$,

(b) $\left[\begin{array}{cc} \sigma \overline{u}_i & g_i \\ g_i^{\mathrm{T}} & R_x \end{array}\right] \geqslant 0 \Leftrightarrow \sigma^2 \overline{u}_i^2 - g_i R_x^{-1} g_i^{\mathrm{T}} \geqslant 0$,

(c) $R_x A_x^{\mathrm{T}} + A_x R_x < 0$,

where g_i is the i-th row of matrix $\left[\begin{array}{c} K_1 L_y(\varepsilon) \\ K_2 L_z(\varepsilon) \end{array}\right]$, which appears in the definition of set F_2 (F_3).

Remark 3. (1) Since optimization problem (33) is of order n_1-dimension and (11) is of order $(n_1+n_2+n_3)$-dimension, the calculation burden is evidently reduced. (2) Since matrix A_x of the constructed system is the system matrix of the slow dynamic system, the reduced-order method avoids the singularity. (3) There is no explicit information about the fast variables $\boldsymbol{y}_1$ and $\boldsymbol{z}_1$ in the estimated stability region except that $\boldsymbol{y}_1$ and $\boldsymbol{z}_1$ are bounded, i.e. the estimated stability region can contain a sufficiently large $\boldsymbol{y}_1$ and $\boldsymbol{z}_1$. Hence, the reduced-order method can reduce the conservatism in the estimation.

Moreover, in the real world, parameter ε may be not sufficiently small and thereby the parameter σ of set F_3 needs to be adjusted to satisfy the conditions in Theorem 2. However, the change of σ has the impact on the optimal solution of optimization problem (31) and optimiza-

tion problem (31) needs to be recalculated with the changed σ. The recalculation inevitably results in redundant calculation. Fortunately, if $\sigma > 0$, we have the following conclusion about optimization problem (31) which can avoid the extra calculation mentioned above.

Lemma 5. For the optimization problem (31), the optimal solution, say, β_x^*, is in proportion to the parameter σ. Namely, if $\sigma'' = \rho\sigma' > 0$ is satisfied, then the corresponding optimal solution satisfies $\beta_x''^* = \rho\beta_x'^*$, where $\rho > 0$ and $\beta_x'^*$ and $\beta_x''^*$ are the optimal solutions of eq. (31) when $\sigma = \sigma'$ and $\sigma = \sigma''$, respectively.

Proof. Readers can refer to ref. [26].

Lemma 5 shows that the optimal solution β^* is in proportion to σ. Therefore, we can choose an arbitrary $\sigma > 0$ when handling optimization problem (31) and use the linear relationship to obtain the β^* corresponding to different σ. Thus it avoids the redundant calculations.

4.2 Algorithm for the reduced-order method

From previous analysis, when matrices L_y and L_z are derived, optimal solution β^* of optimization problem (11) can be easily handled via solving optimization problem (31). However, there is still a difficult problem: though Theorem 2 can guarantee that $L_y(\varepsilon)$ and $L_z(\varepsilon)$ exist when ε is small, the analytical expressions of them are hard to derive. Considering that $L_y(\varepsilon)$ and $L_z(\varepsilon)$ are the smooth functions with respect to ε, we can use Taylor's expression to approximate these two matrixes. Let

$$\begin{cases} L_y(\varepsilon) = L_y^0 + L_y^1\varepsilon + O(\varepsilon^2), \\ L_z(\varepsilon) = L_z^0 + L_z^1\varepsilon + O(\varepsilon^2). \end{cases} \tag{34}$$

Substitute eq. (34) into (12) and compare the order of ε in both sides of the equality, we have

$$\begin{aligned} \varepsilon^0: \quad & A_{21} + A_{22}L_y^0 + (A_{23} + B_2K_2)L_z^0 = 0, \\ & A_{31} + A_{33}L_z^0 = 0, \\ \varepsilon^1: \quad & A_{22}L_y^1 + (A_{23} + B_2K_2)L_z^1 - L_y^0C_0 = 0, \\ & A_{31} + A_{33}L_z^1 - L_z^0C_0 = 0, \end{aligned}$$

where $C_0 = A_{11} + A_{13}L_z^0 + (A_{12} + B_1K_1)L_y^0$.

Solve the above equations and we get

$$L_z^0 = -A_{33}^{-1}A_{31}, \quad L_z^1 = A_{33}^{-1}\left(L_z^0C_0 - A_{31}\right), \tag{35}$$

$$L_y^0 = A_{22}^{-1}\left(A_{23} + B_2K_2\right)A_{33}^{-1}A_{31} - A_{22}^{-1}A_{21}, \tag{36}$$

$$L_y^1 = -A_{22}^{-1}\left(A_{23} + B_2K_2\right)L_z^1 + A_{22}^{-1}L_y^0C_0. \tag{37}$$

Thus from eqs. (35)—(37), we can obtain the first order approximation of the integral manifold. To obtain the more accurate result, high-order approximation results can be applied.

Thus, when ε is small enough, the variables that the reduced-order method needs are all cal-

culated and the algorithm of the reduced-order method is as follows (Algorithm 1):

Step 1: Set up the model as eqs. (2)—(4) and choose the fast variable and the slow variables;

Step 2: Judge whether Assumption 2 is satisfied or not. If they are, then continue; otherwise, use the traditional method to estimate the stability region of the linear system with saturation nonlinearities;

Step 3: Solve eqs. (36)—(37) to obtain the integral manifold, i.e. matrices $L_y(\varepsilon)$ and $L_z(\varepsilon)$;

Step 4: Set up optimization problem (31) and transform it to a simple LMI optimization problem via the changes of eq. (32). Solve this transformed problem and thus β_x^* and the corresponding stability region are derived.

5 Application to power systems

In this section, we will use a test power system with detailed saturated PSS controller models as an example to validate the reduced-order method derived in previous sections.

5.1 The model of PSS with saturated input

Suppose that the power system under study consists of *N* buses and *ng* generators. Without loss of generality, to simplify the expressions in the following analysis, we number the generators in the descending order of H_i, i.e. $H_i \geqslant H_j$ holds when $i < j$.

In order to compare the results in this paper with those of the traditional method in ref. [17], we take the same models as the ones in ref. [17], i.e. the impedance model for loads, the models shown in Figures 3 and 4 for AVR and PSS systems, respectively.

Consider the following saturated constraints:

(1) The output ΔE_f of generator's excitation;

(2) The output y_2 of PSS controller.

Namely, the constrained equations are

$$-\Delta\bar{E}_f \leqslant \Delta E_f \leqslant \Delta\bar{E}_f, \quad -\bar{\boldsymbol{y}}_2 \leqslant \boldsymbol{y}_2 \leqslant \bar{\boldsymbol{y}}_2. \tag{38}$$

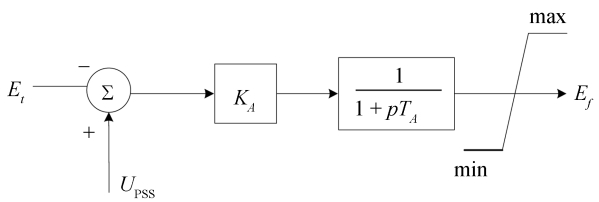

Figure 3 Transfer function of the excitation system.

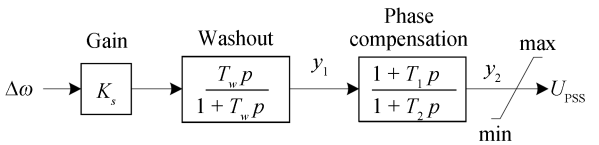

Figure 4 Diagram of the PSS's transfer function.

Consequently, when the saturated inputs are considered, the closed loop system after linearization can be expressed as[17,24]

$$\Delta\dot{\boldsymbol{\delta}} = \Delta\boldsymbol{\omega}, \tag{39}$$

$$\omega_0^{-1} M \Delta\dot{\boldsymbol{\omega}} = -K_1 \Delta\boldsymbol{\delta} - D\omega_0^{-1} \Delta\boldsymbol{\omega} - K_2 \Delta E_q', \tag{40}$$

$$T_{do}' \Delta\dot{E}_q' = -K_4 \Delta\boldsymbol{\delta} - K_3 \Delta E_q' + \text{sat}(\Delta E_f), \tag{41}$$

$$T_A \Delta\dot{E}_{fd} = -K_A K_5 \Delta\boldsymbol{\delta} - K_A K_6 \Delta E_q' - \Delta E_{fd} + K_A \text{sat}(\boldsymbol{y}_2), \tag{42}$$

$$T_w \dot{\boldsymbol{y}}_1 = -K_W K_1 \Delta\boldsymbol{\delta} - K_W D\omega_0^{-1} \Delta\boldsymbol{\omega} - K_W K_2 \Delta E_q' - \boldsymbol{y}_1, \tag{43}$$

$$T_2 \dot{\boldsymbol{y}}_2 = -K_{TM} K_1 \Delta\boldsymbol{\delta} - K_{TM} \omega_0^{-1} D \Delta\boldsymbol{\omega} - K_{TM} K_2 \Delta E_q' + \left(I - T_1 T_w^{-1}\right) \boldsymbol{y}_1 - \boldsymbol{y}_2, \tag{44}$$

where dynamic eqs. (38)—(41) denote the flux decay model of the generators; dynamic eq. (41) is the excitation dynamic model, eqs. (43)—(44) describe the dynamic model for PSS; $K_{TM} = \text{diag}\{T_{1i} K_{si} / M_i\}$, $K_W = \text{diag}\{T_{wi} K_{si} / M_i\}$, $\omega_0 = 2\pi f$, $M = \text{diag}\{2H_i\}$; the variables in eqs. (39)—(44) are partly labeled in Figures 3 and 4, others can be found in ref. [24].

In the excitation system, the constant T_A is very small and the constant K_A is very large. The time constant T_2 is much smaller than T_W in the PSS control system. Hence, for typical parameters as shown in the appendix and observing the time-scale in eqs. (39)—(44), we can find that: ΔE_f and $\boldsymbol{y}_2$ belong to the fast variables; $\boldsymbol{y}_1$, $\Delta E_q'$ and $\Delta\boldsymbol{\delta}$ belong to the slow variables. If H_i is not big enough, $\Delta\omega_i$ belongs to the fast variables category, if H_i cannot be viewed as a small parameter, $\Delta\omega_i$ and $y_{1(i)}$ should be classified to be the slow variables. In the next analysis, without loss of generality, we classify $\Delta\boldsymbol{\omega}$ into slow variables for the simplicity of the following expressions.

Let

$$\boldsymbol{x} = [\Delta\boldsymbol{\delta}^{\mathrm{T}}\ \Delta\boldsymbol{\omega}^{\mathrm{T}}\ \Delta E_q'^{\mathrm{T}}\ \boldsymbol{y}_1^{\mathrm{T}}]^{\mathrm{T}}, \quad \boldsymbol{y} = \Delta E_f, \quad \boldsymbol{z} = \boldsymbol{y}_2. \tag{45}$$

Substitute eq. (45) into eqs. (39)—(44), and the dynamic model is rewritten as

$$\dot{\boldsymbol{x}} = A_{11}\boldsymbol{x} + B_1 \text{sat}(\boldsymbol{y}), \tag{46}$$

$$\varepsilon\dot{\boldsymbol{y}} = A_{21}\boldsymbol{x} + A_{22}\boldsymbol{y} + B_2 \text{sat}(\boldsymbol{z}), \tag{47}$$

$$\varepsilon\dot{\boldsymbol{z}} = A_{31}\boldsymbol{x} + A_{33}\boldsymbol{z}, \tag{48}$$

where

$$A_{11} = -\begin{bmatrix} 0 & -L & 0 & 0 \\ M^{-1}K_1 & M^{-1}D & M^{-1}K_2 & 0 \\ T_{do}'^{-1}K_4 & 0 & T_{do}'^{-1}K_3 & 0 \\ M^{-1}K_s K_1 & M^{-1}K_s D & M^{-1}K_s K_2 & T_w^{-1} \end{bmatrix}; \quad L = \begin{bmatrix} I_{(ng-1,ng-1)} & \vdots & -1 \\ & \vdots & 1 \end{bmatrix};$$

$$B_1 = \begin{bmatrix} 0 & 0 & T_{do}'^{-1} & 0 \end{bmatrix}^{\mathrm{T}}; \quad A_{21} = -\varepsilon T_A^{-1} K_A \begin{bmatrix} K_5 & 0 & K_6 & 0 \end{bmatrix}; A_{22} = -\varepsilon T_A^{-1};$$

$$B_2 = \varepsilon T_A^{-1} K_A; A_{33} = -\varepsilon T_2^{-1}; \quad A_{31} = -\varepsilon T_2^{-1} \begin{bmatrix} K_{TM}K_1 & K_{TM}D & K_{TM}K_2 & (T_1 T_w^{-1} - I) \end{bmatrix}.$$

Obviously, after the change of variables, dynamic systems (46)—(48) can be expressed as systems (2)—(4) studied in previous sections. Moreover, since T_{Ai}, T_{2i} and M_i are all positive

constants, A_{22} and A_{33} are stable matrixes, i.e. the dynamic model of the power system satisfies Assumption 2 and the reduced-order method can be used to estimate its stability region. Moreover, the small parameter ε is embedded in εT_{Ai}^{-1} and εT_{2i}^{-1}, and T_{Ai}^{-1} and T_{2i}^{-1} are small constants. Thus the singularity, due to these small parameters in dynamic systems (46)—(48), is eliminated.

Remark 4. (1) If H_i is not big enough, i.e. M_i is small, the corresponding variable $\Delta\omega_i$ should be classified into the fast variables and y_{1i} should also be classified into the fast variables. However, the dynamic equations corresponding to these two types of variables do not contain the saturation nonlinearities, so these two types of variables can be taken for the part of vector z and the structure of matrix A_{33} is as follows:

$$A_{33} = -\varepsilon \begin{bmatrix} (M^{-1}D)_K & & \\ * & (T_w^{-1})_K & \\ * & * & T_2^{-1} \end{bmatrix}, \tag{49}$$

where $(M^{-1}D)_K$ denotes the diagonal matrix, whose elements are part of $M_i^{-1}D_i$ which are the corresponding generators' parameters classified into the fast variables. (2) If we take the dynamic models such as the motor model for some loads, the corresponding variables may need to be classified into the fast variables. However, it is easy to verify that systems (39)—(44) can still be rewritten as eqs. (46)—(48) and the structure of A_{33} is still like that of eq. (49) except some elements added in the diagonal position. Moreover, if the inertial constants of the loads with the dynamic model are positive, A_{33} is a stable matrix, i.e. Assumption 2 is satisfied so the reduced-order method still works.

5.2 Simulation results

The test power system is composed of 3 generators and 5 buses whose parameters are partly shown in Figure 5. Others are shown in the Appendix. This test system is also studied in ref. [17].

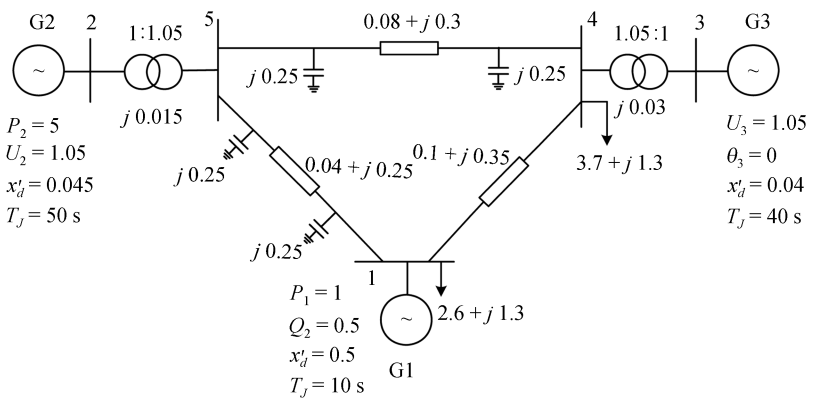

Figure 5 Diagram of the 3-machine, 5-bus system.

5.2.1 Evaluation of the constructed dynamic model. Choose $\varepsilon = 0.1$, $\sigma = 0.95$, and we get the reduced dynamic model via eqs. (36)—(37). For the same initial state, Figure 6 shows the

$\delta - t$ curves and $\omega - t$ curves of the reduced-order system and the primary high-order system, respectively. Figure 7 shows that the fast variables approach the integral manifold rapidly.

In Figure 6, for the slow variables such as the angles and the derivatives of the angle of the generators, we can find that the error between the reduced-order dynamic system and the primary high-order dynamic system is very small and is evanescent as time increases. This result is in accordance to the conclusion in Theorem 1. Hence, the impacts of fast variables on the slow variables can be ignored for this case. In other words in this test system, the small parameter satisfies the conditions which Theorem 1 needs.

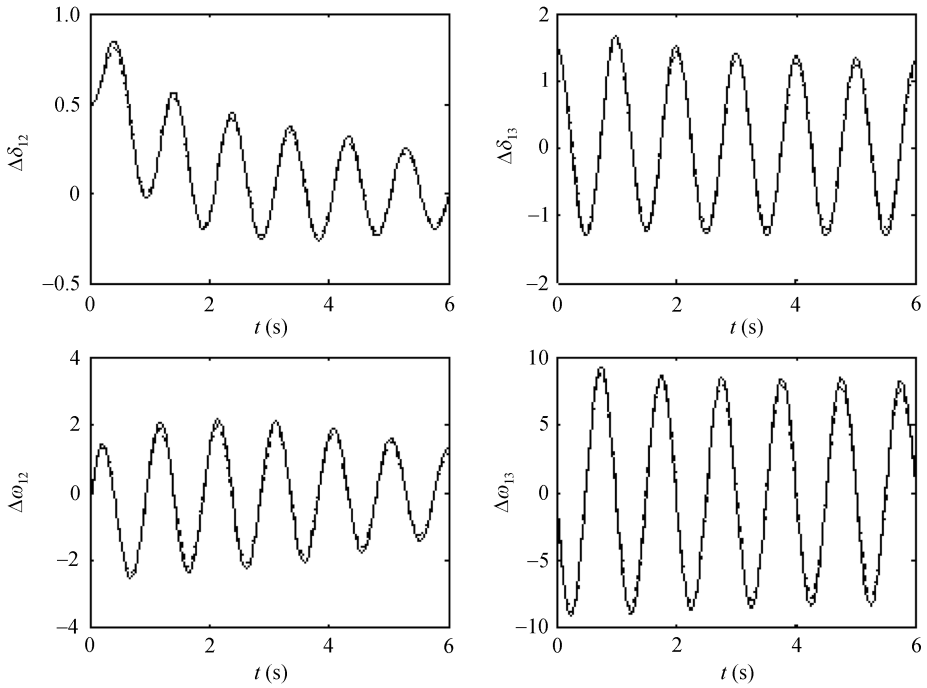

Figure 6 Results of the high-order system and the reduced-order system in the time domain. ——, Trajectories of the reduced-order system; ------, trajectories of the primary high-order system.

From Figure 7, we can find that the decay speeds of fast variables are much rapid compared to those of the integral manifolds made up of the slow variables. It also can be found that 0.5 seconds later, the fast variables have by and large converged to the integral manifolds. This phenomenon validates the conclusions in Lemma 1 in which the fast variables converge to the corresponding integral manifolds with time-scale t/ε. Moreover in the same time-scale, we can explain this phenomenon from the viewpoint of the eigenvalues, i.e. the eigenvalues to which the fast variables corresponding are much smaller than the eigenvalues to which the slow variables are corresponding. This result is illustrated in Table 1, where the eigenvalues of the reduced-order dynamic system and of the high-order dynamic system are shown.

In Table 1, the distribution of eigenvalues of the reduced system is much evener than that of the high-order system. This phenomenon indicates that the reduced-order method can alleviate the singularity of the high-order dynamic system. From this table, we also can see that the reduced-order system preserves the small eigenvalues which correspond to the slow modes (the

modes associated with the δ and ω terms of the generators). Hence, the reduced-order method does not lose the oscillation modes of slow variables, i.e. electromechanical oscillation modes, but ignores the fast variables of global stability. Moreover, this conclusion implies that the classification of the test power system under study is correct.

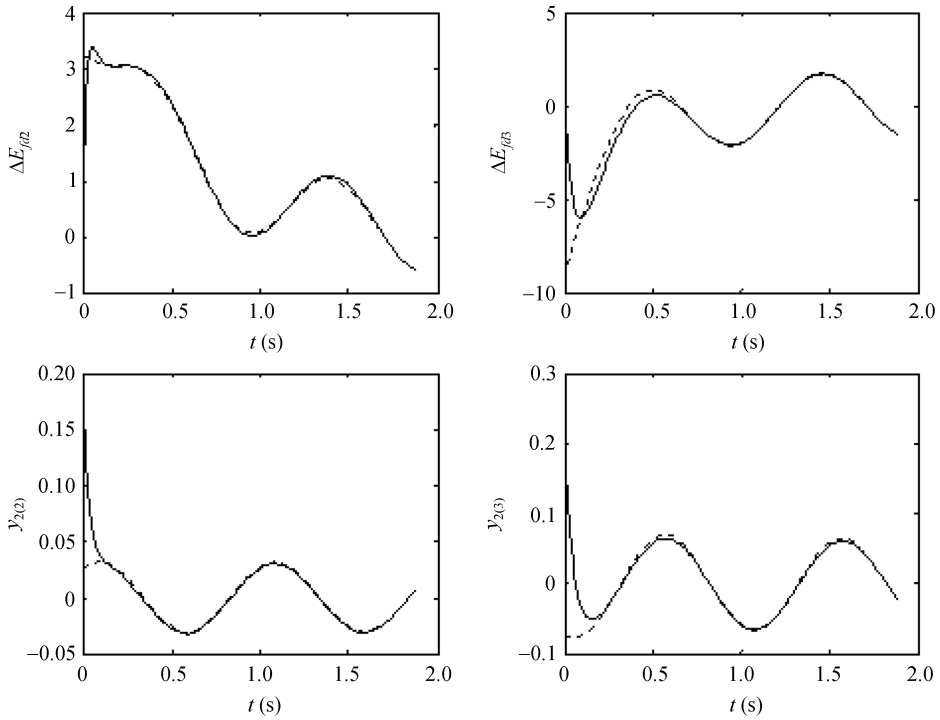

Figure 7 Figures of fast variables converging to the integrated manifolds. ——, Trajectories of the reduced-order system; -----, integral manifolds.

Table 1 Eigenvalues of the high-order system and the reduced-order system

Eigenvalues of the primary system	Eigenvalues of the reduced-order system
–49.8653, –48.6570, –46.3741, –33.2216, –33.0554, –18.5341	—
–4.8264, –1.8397	–4.6831, –1.8353
–0.6689, –0.3899, –0.1217, –0.1889	–0.6687, –0.3917, –0.1217, –0.1889
–0.0595±6.7262i, –0.1506±6.2715i	–0.0610±6.7269i, –0.1706±6.2615i

5.2.2 Results based on the reduced-order method. The analysis of theory and simulation all show that the reduced-order dynamic system can approximate the primary high-order dynamic system well. In this subsection, we will show that the optimization results based on the reduced-order method are also correct.

To compare the results of the reduced-order method with those of the traditional high-order method, we also consider that the set containing the expected initial states is the hyper-ball studied in ref. [17]. It should be noted that, due to renumbering the generators, the referenced machine of this paper is the first machine of the Appendix and in ref. [17] the referenced machine is the third machine. Moreover, $\Delta\omega$ in this paper is a nominal variable. In ref. [17], this variable is a per-unit value. Hence, if we let $\boldsymbol{\xi}=[\Delta\delta_{21},\Delta\delta_{31},\Delta\omega_{21},\Delta\omega_{31},\cdots]^{\mathrm{T}}$ and $\boldsymbol{\xi}'=[\Delta\delta_{13},\Delta\delta_{23},$

$\Delta\omega'_{13}, \Delta\omega'_{23}, \cdots]^{\mathrm{T}}$ denote the states of the dynamic system of this paper and those of ref. [17], then we have $\boldsymbol{\xi}' = H\boldsymbol{\xi}$ and the set containing the expected initial states can be denoted by $E(H^{\mathrm{T}}H, 1) = \{\boldsymbol{\xi} \mid \boldsymbol{\xi}^{\mathrm{T}} H^{\mathrm{T}} H \boldsymbol{\xi} \leqslant 1\}$, i.e. in expression (10) P'_0 satisfies $P'_0 = H^{\mathrm{T}}H$. Here, H is defined as $H = \mathrm{diag}\left\{\begin{bmatrix} 0 & -1 \\ 1 & -1 \end{bmatrix}, \omega_0^{-1}\begin{bmatrix} 0 & -1 \\ 1 & -1 \end{bmatrix}, I\right\}$.

We can get the initial set with reduced order by eq. (28) and Lemma 3. We can get the optimal solution $\beta_x^* = 7.95 \times 10^{-2}$ of eq. (31) by Algorithm 1 developed in section 4 based on the high-order dynamic system, if the optimal solution is $\beta^* = 8.22 \times 10^{-2}$. Hence, for this case, the reduced-order method brings a small error, which also can be indicated by Figure 8, where the ellipses enclosed by the real lines and by the dash lines are the projections of the stability region based on the high-order dynamic system and the reduced-order method, respectively. In this figure, we can find that there are very small differences between the projections on the coordinates of slow variable $\Delta\delta$ and $\Delta\omega$ of the estimated stability region based on the high-order system and those based on the reduced-order system.

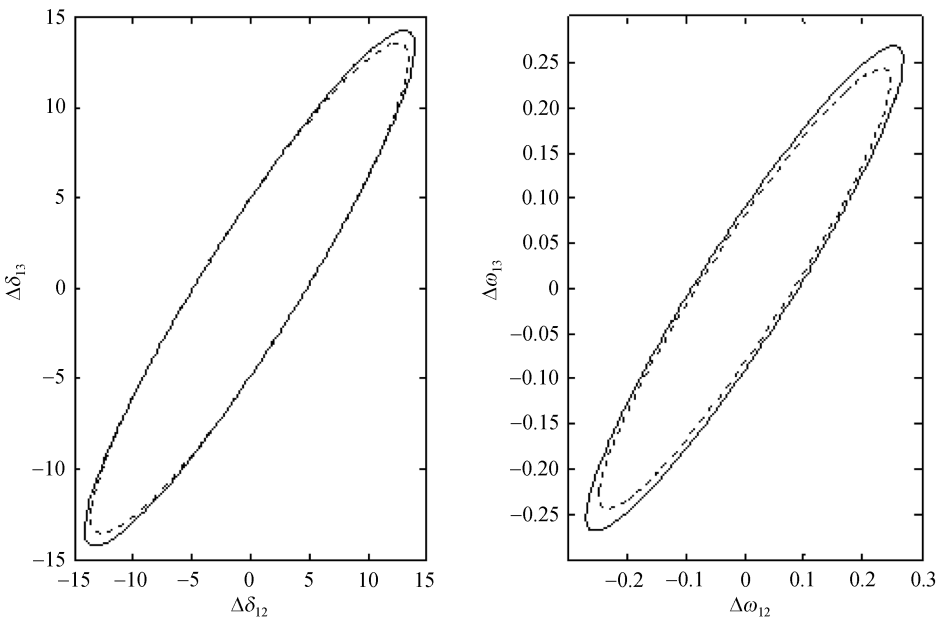

Figure 8 Projections of the attractive regions of the high-order and the reduced-order system. ——, Projection of the stability region of high-order system; ------, projection of the stability region of reduced-order system.

In Figure 8, the projections on the coordinates of the slow variables are almost overlapped. However, from Theorem 2, we can get that the projections of the estimated stability region, via reduced-order method, on the coordinates of the fast variables are the global state space. Moreover, the corresponding projections of the stability region via the high-order method in ref. [17] are the areas enclosed by the ellipses as shown in Figure 9. In other words, the reduced-order method alleviates the conservation in the estimation since the method has used an underlying conclusion that fast variables converge to the corresponding integral manifolds globally.

If the expected initial states can be contained in a low dimension ellipse, say X'_0, which is

independent of the slow variables, i.e. P_0' has the structure as $P_0' = \mathrm{diag}\{0, P_{22}^0\}$ in eq. (10), then from Theorem 2 we know that the estimated stability region can contain a large enough X_0' by the reduced-order method. Clearly, this conclusion cannot be drawn by the high-order method. However, this conclusion is important since it implies that under certain conditions in power systems, we need not pay much attention to the impact of the transient disturbance on the fast variables such as ΔE_{fd} and y_2 which are variables of the generator's controls.

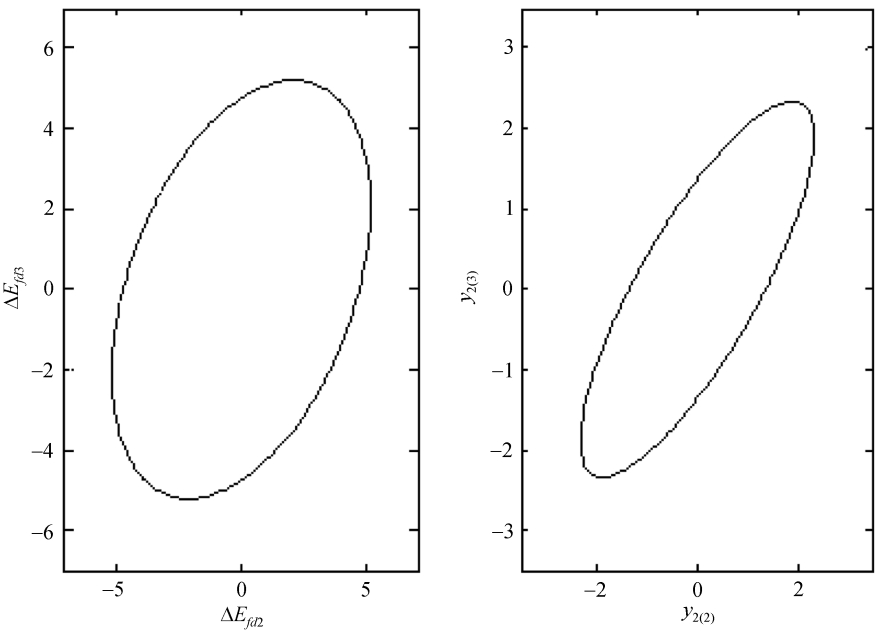

Figure 9 Projections of the stability region based on the high-order system.

6 Conclusion

For a singular system with saturation nonlinearities, a reduced-order method is suggested based on the singular perturbation theory. The traditional methods for estimating the stability region of the singular, high-dimension system with saturation nonlinearities will meet with some difficult problems such as a heavy calculation burden, singularity and conservatism, etc. These problems can be solved to some extent by the method proposed in this paper. The reduced-order method was applied to test power systems with the saturated PSS controllers. Simulation results indicated the effectiveness of the method.

Appendix

In this appendix, we give the parameters of the generators, the PSS systems and the exciter's control systems in Figure 5.

Generator 1:

$P_1 = 1, \quad Q_1 = 0.5, \quad x_d' = 0.5, \quad H = 5\ \mathrm{s}, \quad D = 0.005, \quad T_{do}' = 5.35; \quad K_A = 6, \quad T_A = 0.02\ \mathrm{s};$

$K_s = 1.0,\quad T_w = 5.0\text{ s},\quad T_1 = 0.35\text{ s};\quad T_2 = 0.03\text{ s};\quad \Delta\overline{E}_{f1} = 6.2,\quad \overline{y}_2 = 3.0.$

Generator 2:

$P_2 = 5,\quad U_2 = 1.05,\quad x'_d = 0.045,\quad H = 25\text{ s},\quad D = 0.025,\quad T'_{do} = 5.35;\quad K_A = 10,\quad T_A = 0.02\text{ s};$

$K_s = 1.0,\quad T_w = 8.3\text{ s},\quad T_1 = 0.35\text{ s},\quad T_2 = 0.03\text{ s};\quad \Delta\overline{E}_{f1} = 5.2,\quad \overline{y}_2 = 3.0.$

Generator 3:

$\theta_3 = 0,\quad U_3 = 1.05,\quad D = 0.020,\quad H = 20\text{ s},\quad x'_d = 0.04,\quad T'_{do} = 3.76;\quad K_A = 17.5,\quad T_A = 0.02\text{ s};$

$K_s = 1.0,\quad T_w = 8.0\text{ s},\quad T_1 = 0.45\text{ s},\quad T_2 = 0.05\text{ s};\quad \Delta\overline{E}_{f1} = 5.2,\quad \overline{y}_2 = 3.0.$

1 Hu T, Lin Z, Chen B M. An analysis and design method for linear systems subject to actuator saturation and disturbance. Automatica, 2002, 38(2): 351－359

2 Hindi H, Boyd S. Analysis of linear systems with saturation using convex optimization. In: Proceedings of the 37th IEEE Conference on Decision & Control. New York: Piscataway NJ, 1998. 903－908

3 Cao Y, Lin Z, Ward D G. An anti-windup approach to enlarging domain of attraction for linear systems subject to actuator saturation. IEEE Trans Autom Contr, 2002, 47(1): 140－145

4 Crow M L, Ayyagari J. The effect of excitation limits on voltage stability. IEEE Trans Circ Syst-I, 1995, 42(12): 1022－1026

5 Ji W, Venkatasubramanianian V. Hard-limit induced chaos in a fundamental power system model. Intern J Electr Power Energy Syst, 1996, 18(5): 279－295

6 Escarela-Perez R, Niewierowicz T, Campero-Littlewood E. A study of the variation of synchronous machine parameters due to saturation: A numerical approach. Electr Power Syst Res, 2004, 72(1): 1－11

7 Xi Z, Feng G, Cheng D, et al. Nonlinear decentralized saturated controller design for power systems. IEEE Trans Contr Syst Tech, 2003, 11(4): 539－547

8 Gan D Q, Qu Z H, Cai H Z. Multi-machine system excitation control via theories of feedback linearization control and nonlinear robust control. Inter J Syst Sci, 2000, 31(4): 519－527

9 Yu Y X, Jia H J, Wang C S. Chaotic phenomena and small signal stability region of electrical power systems. Sci China Ser E-Tech Sci, 2001, 44(2): 187－199

10 Rajkumar V, Mohler R R. Nonlinear control methods for power systems: A comparison. IEEE Trans Contr Syst Tech, 1995, 3(2): 231－237

11 Lu Q, Sun Y Z, Mei S W. Nonlinear Control Approach and Implementation in Power System Dynamics. Boston: Kluwer Academic Publishers, 2001. 68－76

12 Hu T, Lin Z. Control Systems with Actuator Saturation: Analysis and Design. Boston: Birkhauser, 2001. 157－191

13 Dobson I, Lu L. Voltage collapse precipated by the immediate change in stability when generator reactive power limits are encountered. IEEE Trans Circ Syst-I, 1992, 39(9): 762－766

14 Gutman P O, Hangander P. A new design of constrained controllers for linear systems. IEEE Trans Autom Contr, 1985, 30(1): 22－33

15 Venkatasubramanian V. Stability boundary analysis of nonlinear dynamics subject to state limits. In: Proceedings of the 34th Hawaii International Conference on System Science. Los Alamitos: IEEE Computer Society, 2001. 1－6

16 Hu T S, Lin Z L. Exact characterization of invariant ellipsoids for single input linear systems subject to actuator saturation. IEEE Trans Autom Contr, 2002, 47(1): 164－169

17 Xin H, Gan D, Chung T S, et al. A method for evaluating the performance of PSS with saturated input. Electr Power Syst Res, 2007, 77(10): 1284－1291

18 Tse C T, Wang K W, Chung C Y, et al. Robust PSS design by probabilistic eigenvalue sensitivity analysis. Electr Power Syst Res, 2001, 59(1): 47－54

19 Kokotovic P V, Khalil H K, O'Reilly J. Singular perturbation methods in control: Analysis and design. London: Academic

Press, 1986. 47－68
20 Singh H, Brown R H, Naidu D S, et al. Robust stability of singularly perturbed state feedback systems using unified approach. IEE Proc Contr Theory Appl, 2001, 148(5): 391－396
21 Kundur P. Power system stability and control. New York: McGraw-Hill, 1994. 315－335
22 Liu Y Q, Yan Z, Ni Y X. Study on the order reduction of two-time scale power system dynamic models. I. Power system singular perturbation model. Autom Electr Power Syst (in Chinese), 2002, 26(18): 1－5
23 Hu T S, Lin T L. Exact characterization of invariant ellipsoids for single input linear systems subject to actuator saturation. IEEE Trans Autom Contr, 2002, 47(1): 164－169
24 Ni Y X, Chen S S, Zhang B L. Theories and Analysis of Dynamic Power Systems (in Chinese). Beijing: Tsinghua University Press, 2002. 235－251
25 Khalil H K. Nonlinear Systems. 2nd ed. New Jersey: Prentice Hall, 1996. 78－81
26 Xin H H. An study on the impact of parameter uncertainties and saturation nonlinearities on power system stability. Doctoral Dissertation (in Chinese). Hangzhou: Zhejiang University, 2007. 97－123